

Structure of a Muramic Acid Containing Capsular Polysaccharide from the Pathogenic Strain of *Vibrio vulnificus* ATCC 27562.

Shamantha Gunawardena¹, G. P. Reddy¹, Yuhui Wang¹,
V.S. Kumar Kolli², Ron Orlando², J. Glenn Morris³ and C. Allen Bush^{*1}

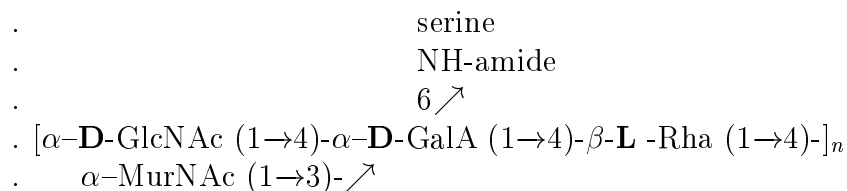
1. Department of Chemistry & Biochemistry,
University of Maryland Baltimore County, Baltimore, MD 21250.
2. Complex Carbohydrate Research Center and Department of Biochemistry and Molecular Biology
The University of Georgia 220 Riverbend Road Athens, GA 30602-4712
3. Departments of Medicine and Pathology,
University of Maryland School of Medicine and Veterans Affairs Medical Center, Baltimore, MD 21201.

Research supported by NSF Grant MCB 91-05586 to C.A.B. and by a grant from the Department of Veterans Affairs to JGM.

* Corresponding author – ph. (410) 455-2506, fax (410) 455-2608, e-mail bush@umbc.edu

Abstract

Vibrio vulnificus strains isolated from septicemia cases as well as from the environment show a wide variety of capsular types. In an attempt to find common structural features which can be correlated with pathogenicity and toxicity, we have determined structures of the capsular polysaccharides from several pathogenic strains. We report the complete structure of the polysaccharide from the pathogenic *V. vulnificus* strain ATCC 27562 using a combination of homonuclear and hetero nuclear one-dimensional and two-dimensional NMR experiments. The ^{13}C and ^1H NMR spectra including the exchangeable amide proton resonances have been completely assigned. The amide linkage between Ser and C6 of GalA has been unambiguously determined by water suppressed 2D NOESY. To verify the structure established by NMR, we have fragmented the polymer employing the Smith degradation procedure. The Smith product identified by NMR and matrix assisted laser desorption mass spectrometry is consistent with the proposed structure for the CPS which is composed of D-GlcNAc, MurNAc, D-GalA, L-Rha and serine linked as shown:



1. Introduction

Vibrio vulnificus is a Gram-negative bacterial pathogen which is among the most common free-living bacteria in estuarine environments [1]. It is frequently present in filter-feeding shellfish, such as oysters, which have been harvested during warm summer months when *V. vulnificus* is present in the highest numbers in water. The organism can cause serious human infections when it contaminates a seawater-exposed wound. Persons who eat raw oysters containing the bacterium, and who have underlying liver disease or who are immunosuppressed, are at risk for development of primary septicemia. Mortality rates for persons with primary septicemia exceed 50%, with patients developing intractable shock and multi-organ system failure despite aggressive medical care and antimicrobial therapy. *V. vulnificus* produces a capsular polysaccharide which is essential for virulence [2]. This capsule provides the bacterium with resistance to serum bactericidal activity and phagocytosis; the capsular material has also been shown to directly stimulate the release of TNF α (tumor necrosis factor α) and other cytokines from peripheral blood mononuclear cells [3]. Capsular polysaccharide-protein conjugate vaccines provide protection against lethal infection in mouse models [4]. Antibodies raised to the purified capsular material are also protective, both prior to and after challenge with a fully virulent *V. vulnificus* strain. However, protection is provided only against strains of the homologous capsular type [5].

In earlier studies we have shown a variety of capsular types among *V. vulnificus* strains. The first reported structure was that of strain MO6-24 [6]. It has subsequently been shown by reaction with antibodies raised to protein conjugates and by carbohydrate analysis of the capsules that *V. vulnificus* has multiple capsular types [7,8]. We have reported the structure of the CPS

(capsular polysaccharide) of another pathogenic strain, BO63216 which is similar to that of strain MO6-24 but can be readily distinguished by both chemical and immunological methods [9]. In the present work we report the complete structure of the CPS of another pathogenic strain ATCC27562 which differs more fundamentally in structure from that of strain MO6-24.

We have recently carried out an extensive survey of over 100 environmental isolates of *V. vulnificus* using a simplified HPAEC (high performance anion exchange chromatography) method for approximate carbohydrate analysis of the capsule to assign a 'carbotype' to each strain [10]. This crude method was used to distinguish 94 carbotypes from a collection of 120 strains illustrating the wide variety of different capsule structures present in the environment. At present it is not known whether there is a correlation between capsule type and pathogenic potential. Examination of the existing data on carbohydrate analysis of the capsules does not reveal any obvious correlation and few detailed structures are known. Since it appears that the capsular polysaccharide of the pathogenic strain, MO6-24, interacts directly with the immunological system, knowledge of a number of different polysaccharide structures will be valuable to establish correlations with activation of peripheral blood mononuclear cells [3]. Success in establishing such correlations could lead to proposals for chemical structures which can block those interactions and form a basis for drug therapy of septicemia cases.

2. Materials and Methods

Single bacterial colonies grown from frozen glycerol stocks were inoculated into L-broth for 18 h growth at 30° C . A 1 mL aliquot of each culture was spread on L-agar in 28 × 48-cm pans and incubated overnight at 30°C. Cells from two pans were harvested and suspended in 80 mL of phosphate-buffered saline. Bacteria were shaken at 200 rpm on a rotary shaker in 250-mL baffled

polystyrene bottles for 30 min at room temperature. Cells and debris were removed by centrifugation (16,000 x g, 20 min, 4°C), and supernatants were dialyzed with multiple changes of distilled water and concentrated about twofold by ultrafiltration (10,000-nominal molecular weight stirred cell; Amicon, Beverly, Mass.). The retentates were then ultracentrifuged (154,000 x g, 16 h, 20°C), and the supernatants were removed and subjected to enzymatic digestion with RNase A (100 µg/mL), DNase I (50 µg/mL plus 1 mM MgCl₂), pronase (250 µg/mL) followed by sequential phenol-chloroform extraction. The aqueous layer was dialyzed as described above, and the resultant sample was lyophilized.

12.0 mg of *Vibrio vulnificus* ATCC 27562 capsular polysaccharide was passed through a Dowex 50W-X8(30x1.0cm) cation-exchange resin (H⁺ form) column, and was eluted with water. Fractions containing polysaccharide were monitored by UV absorbance at 205 nm, pooled, freeze dried, dissolved in 1.0 mL of deionized water and incubated at 80/degC for 10 h. The sample was run through a P6-column (100x2cm) using water for elution, and the fractions at the void volume containing polysaccharide were collected and freeze dried. This sample was used for NMR experiments and carbohydrate analysis.

Carbohydrate Analysis: 200 µg of sample was hydrolyzed in 4 M HCl (200 µL) for 8 h at 100° C . Acid was evaporated with dry nitrogen gas, then the residue was dissolved in 200 µL of distilled water and run through a 0.22 µm Millipore filter. An 800 µg sample of *Proteus penneri* strain 19 O-specific polysaccharide (a gift from Dr. Knirel) was hydrolyzed with 2 M TFA at 120 ° C for 2 h, dried, and the residue was dissolved in 800 µL of distilled water to provide a chromatographic standard for isomuramic acid [11]. Other HPAEC standard sugars included GlcNAc, muramic acid, rhamnose and galacturonic

acid.

HPAEC was carried out on a Dionex Glycostation equipped with an autosampler. 20 μL samples were injected onto a CarboPAC PA-1 column which was eluted at a flow rate of 1.0 mL/min with several different protocols, three of which are suitable for detection of acidic sugars and one of which is suitable for neutral and amino sugars [12]. Neutral sugars were eluted with 16 mM NaOH while 100 mM NaOH plus 150 mM NaOAc, 100 mM NaOH plus 75 mM NaOAc and 50 mM NaOH plus 150 mM NaOAc were used to elute acidic sugars (Table 1). The analysis was followed by a 15 min rinse with NaOAc and NaOH, then the column was equilibrated with the running solvent for 15 min before a new sample was injected.

Amino Acid Analysis: 10 μg of sample was hydrolyzed with HCl vapor at 110° C for 24 h, the hydrolysate was derivatized with phenyl isothiocyanate to give PTH (phenylthiohydantoin) amino acids, and was separated by reversed phase HPLC; a separate analysis was carried out with another aliquot of 25 μg of sample. These were done by Analytical Biotechnology Services (Boston, MA).

Smith Degradation: 20 mg of capsular polysaccharide in 1.5 mL of H₂O was thoroughly mixed with 1.5 mL of NaIO₄ (0.12M) and was oxidized in the dark at 4° C for six days. Excess periodate was decomposed by the addition of 125 μL of 10% ethylene glycol, then allowed to stand for 4 h, and the oxidized polysaccharide was reduced with NaBH₄ (50 mg) for 24 h. Excess NaBH₄ was decomposed by dropwise addition of 5 M HCl until the mixture was mildly acidic (pH 5.5). Carbohydrate analysis on a 200 μL of the mixture (hydrolysis by 4 M HCl, 100° C , 6 h) was carried out to test the completeness of oxidative cleavage. The remainder of the sample was lyophilized, dissolved in 1 mL of distilled water, filtered through a 0.45 μm Millipore filter, and

was applied to a BioGel P-6 Gel column (2.5×85cm) for desalting, using H₂O as the eluant. 4 mL fractions were collected and absorbance at 205 nm was monitored. Fractions containing polysaccharide at the void volume were pooled, freeze dried, hydrolyzed with 0.5 M TFA (2 mL) at 65° C for 100 min, and dried to remove acid. The product was dissolved in 700 μL H₂O, loaded on a Bio-Gel P-2 column (1.2×120cm) and eluted with H₂O. 1.1 mL fractions were collected and the fractions yielding absorbance at 205 nm in the included volume were pooled and freeze dried. This Smith oligosaccharide (SMOS) sample (yield 8 mg) was used for carbohydrate analysis, NMR and mass spectroscopic studies.

Nuclear Magnetic Resonance Spectroscopy:

Capsular polysaccharide as well as the Smith oligosaccharide was exchanged thrice with 99.9% D₂O before dissolving in 500μL of 99.96% D₂O for NMR experiments. All experiments with the CPS were carried out at a probe temperature of 50° C , and at 30° C for the SMOS. For water suppressed experiments, samples were dissolved in 500μL solution of TFA (pH 3.0) and D₂O mixed in a ratio of 9:1. All water suppressed experiments and experiments with SMOS were recorded at a proton frequency of 500 MHz on a General Electric Omega-500 PSG system, while a GN-500 spectrometer was used for the CPS experiments. The reported chemical shifts are shown relative to internal sodium-4,4-dimethyl-4-silapentane-1-sulfonate (DSS) using acetone as a secondary standard (2.225 ppm for ¹H and 31.07 ppm for ¹³C downfield from DSS). All 2D NMR data sets were acquired without sample spinning in the phase sensitive mode. DQF COSY, NOESY and HOHAHA spectra were recorded using standard pulse sequences. Magnetization was locked with a B₁ field of 9 kHz for 70 ms isotropic mixing time in HOHAHA [13-14] and a mixing time of 60 ms was used for NOESY.

An HMQC (heteronuclear multiple quantum coherence) [15] spectrum was acquired both with and without decoupling at the carbon frequency during acquisition. HMBC (heteronuclear multiple bond correlation) was recorded using the pulse sequence of Bax and Summers [16]. A carbonyl selective HMBC (SELMHBC) with a 60 ms delay to develop heteronuclear multiple quantum coherence was recorded by shifting the ^{13}C carrier frequency down field by 114 ppm (relative to HMQC and HMBC) together with a 400 μs soft carbon pulse to excite only the carbonyl carbon resonances.

Proton 1D, NOESY and HOHAHA data in 9:1 H_2O and D_2O were recorded using water suppression by presaturation. The carrier was kept on H_2O resonance and was saturated for 800 ms with a Dante pulse train consisting of 5° pulses separated by 100 μs intervals [17] followed by a 30 ms SCUBA delay period [18] to recover the resonances closer to the H_2O peak.

A similar set of experiments were recorded for the SMOS at 30°C . Additionally, a series of HOHAHA experiments were done with spin lock mixing times of 10, 20, 40, 60 and 80 ms to observe the progression of through-bond magnetization transfer along each spin system. All NMR data were processed off line on a Silicon Graphics workstation using Felix 2.3 program.

Gas Liquid Chromatography:

GLC was performed with a Shimadzu GC 14A gas chromatograph equipped with a flame ionization detector and a glass capillary column (10 m \times 0.54 mm) with a wall coated with AT-35. The carrier gas was nitrogen and the flow rate was 1 mL/min. 20 μg of standard sugars (D-galacturonic acid, N-acetyl-D-glucosamine, L-rhamnose, muramic acid and N-acetyl-muramic acid) were butanolysed with 50 μL of (\pm)-2-butanolic HCl (1 M) for 8 h at 80°C . After evaporating the excess solvent, they were silylated with 50 μL of trimethylsilylation reagent (TMS) composed of hexamethyl disilazane,

chlorotrimethylsilane in pyridine (1:1:3 by volume). Experiments using S-(+)-2-butanol and R-(-)-butanol were performed under the same conditions. Similarly, 20 μg of CPS was butanolysed and silylated under the same conditions prior to GLC analysis.

Mass Spectrometry:

The MALDI mass spectra were run on the MS1 unit of a JEOL (Japan) SX/SX 102A mass spectrometer fitted with a point detector. The mass spectrometer was calibrated with FAB before the attachment of laser equipment for MALDI using an external standard of an alkali-iodide mixture [19]. A nitrogen laser of 337 nm wavelength, 3 ns pulse width and a pulse rate of 20 Hz was used for MALDI analysis. An aliquot of 1 μL of carbohydrate (about 100 pmol) was mixed with 5 μL of matrix (α -cyano-4-hydroxycinnamic acid and 3-aminoquinoline) [20-21] and the mixture was loaded onto the FAB probe tip. Collisional induced dissociation (CID) was performed in the first field free region of MS1 using helium as a collision gas and the pressure of the gas was adjusted for 50% attenuation of precursor ion. The CID spectrum was acquired in B/E mode at a rate chosen to scan the mass range 5-2000 in 1 min with a filtering of 300 Hz and the spectrum is an averaged profile of about 20 scans.

3. Results

The ^1H NMR spectrum (not shown) of *V. vulnificus* ATCC 27562 CPS in D_2O contains eight resonances in the downfield anomeric region (between 4.2 and 5.3 ppm). Also the high-field methyl region contains four signals, two of which (2.12 ppm and 2.02 ppm) are singlets characteristic of N-acetyl methyl groups. However, the anomeric region of the HMQC spectrum (Fig. 1) shows only four cross peaks indicating the presence of only four sugar residues in the repeating subunit.

In the analysis of the acid hydrolysate of the polysaccharide by HPAEC using the elution protocol for neutral sugars, [6] two peaks were identified, one corresponding to rhamnose (8.6 min) and one to glucosamine (12.2 min). The results of NMR spectroscopy, to be discussed below, are consistent with the presence of these two monosaccharides and also suggested galacturonic acid and muramic acid as component monosaccharides. HPAEC gave peaks corresponding to these two monosaccharides under elution conditions suitable for acidic sugars. It was not certain that our NMR methods, to be described below, could discriminate between muramic acid and isomuramic acid, 3-O-(S)-1-carboxyethyl D-GlcNAc. Therefore we also analyzed the hydrolysate of the O-polysaccharide from *Proteus penneri* strain 19 which has been reported to contain isomuramic acid along with galactose and N-acetyl glucosamine in the repeating unit. The HPAEC data (Table 1) show that muramic acid can be readily discriminated from isomuramic acid by this method as does cation exchange chromatography as reported by Knirel and coworkers [11]. Although isomuramic acid elutes much later than muramic acid when eluted with 100 mM NaOH and 150 mM NaOAc, it runs very close to galacturonic acid under these elution conditions. However, excellent separation of all three of these acidic sugars could be observed with 100 mM NaOH and 75 mM NaOAc as indicated in Table 1, establishing galacturonic acid and muramic acid unambiguously.

Since NMR results to be discussed below suggested the presence of an amino acid in the structure, amino acid analysis was carried out by reverse phase HPLC and serine was the only amino acid detected.

Complete assignment of the ^1H spectrum was carried out by ^1H correlation using DQF-COSY and TOCSY spectra (data not shown). Using these together with a series of heteronuclear NMR experiments [22] complete struc-

tural information such as linkage, anomeric configuration, residue types and their ring sizes were obtained. Spin systems each representing a residue were identified by lower case boldface letters as indicated in the proposed structure of the polysaccharide given in Scheme 1.

Both **a** and **d** spin systems were found to be of the *gluco* configuration from estimates of the homonuclear coupling constants in DQF-COSY and HOHAHA spectra (not shown). Because large coupling constants favor almost complete magnetization transfer throughout the spin-system, the partial sub-spectrum across the anomeric proton resonance (4.45 ppm) on the diagonal of 2D HOHAHA spectrum (not shown) shows cross peaks to all proton resonances up to H6 (Table 2), consistent with a glucopyranose residue [23]. Similar observations for residue **a** indicate its *gluco* configuration. All ^{13}C resonance assignments were obtained directly from one bond HMQC correlations of attached protons and were independently confirmed by the many intra-residue HMBC connectivities observed, as shown in Fig. 2. ^{13}C chemical shifts of C2 of both **a** and **d** are typical of amino sugars (see Table 3) and the two H6 methylene resonances of both are strongly coupled as seen in the HMQC spectrum (Fig. 1). Though there was an overlap of **d** H2 and **d** H6 in the HOHAHA spectrum, assignment was made by the HMBC correlation to **d** H2 from both **d** C1 and **d** C3. The quartet at 4.59 ppm and the methyl doublet at 1.41 ppm, which are correlated in DQF-COSY, were assigned to H2' and H3' of a 1-carboxy-ethyl moiety as HOHAHA intensities were not observed from either one of them to any other resonances (Table 2). H2' in this spin system shows HMBC correlation to C3', and H3' is correlated to C2' and C1' as shown in Fig. 2. Also, the HMBC spectrum shows that H2' correlates with C3 of residue **a** and that C2' is correlated with H3 of the same residue proving that the 1-carboxy-ethyl is linked to **a** at C3. Thus **a** is the

muramic acid and residue **d** is the GlcNAc identified in the HPAEC analysis. NOE correlation between **a** H3 and **a** H2' previously reported by others [24] for muramic acid, was also observed in NOESY (Table 2). $^1J_{C1H1}$ measured from coupled HMQC for **d** is small (Table 3) indicating the β -configuration [25]. The large $^3J_{H1-H2}$ (Table 3) and the NOE peaks from **d** H1 to **d** H3 and **d** H5 shown in Fig. 3 are consistent with this configuration. In contrast, $^1J_{C1H1}$ of residue **a** is large, the $^3J_{H1-H2}$ is small and intra residue NOE correlation from **a** H1 is found only to **a** H2 indicating the muramic acid to be an α -sugar.

From **b** H1 at 5.19 ppm the spin system could be traced only up to H4 from both DQF-COSY as well as HOHAHA. NOESY (Fig. 3) however shows a strong cross peak between H3 and H5; also H4 at 4.21 ppm shows NOE to both H3 and H5 as observed in galactopyranosides. From the cross peak patterns of DQF-COSY, $^3J_{H2-H3}$ was found to be much larger (~ 9 - 10 Hz) than both $^3J_{H1H2}$ and $^3J_{H3H4}$ (~ 3 - 4 Hz). However, the H4/H5 cross peak was extremely weak in DQF-COSY, indicating a very small coupling constant between these two resonances, as is generally observed for *galacto* type sugars. A strong HMBC cross peak between **b** H1 and C5 of that residue is characteristic of pyranosides with the α -configuration. H6 for spin system **b** was not found either in DQF-COSY or HOHAHA. However, **b** H5 at 4.73 ppm shows a correlation with a carbonyl carbon resonance at 171.20 ppm in a SELHMBC experiment (not shown) indicating C6 of a uronic acid, thus establishing residue **b** to be galacturonic acid consistent with the HPAEC data. $^1J_{C1-H1}$ and $^3J_{H1H2}$ values in Table 3 indicate its α anomeric configuration.

Signals characteristic of a methyl group of a 6-deoxy sugar in spin system **c** identify it as rhamnose as the 1H coupling constants are characteristic of the

manno configuration. The anomeric configuration of rhamnose was identified as β from its small $^1J_{C_1H_1}$ value (Table 3) and large NOE cross peaks from H1 to H3 and H5 (Fig. 3).

Difficulties in assignment due to 1H and ^{13}C resonance overlaps were overcome by long range heteronuclear connectivities. Because single bond (^{13}C - 1H) correlations **a** 5 and **d** 3 were found overlapped in HMQC (Fig. 1), long-range connectivities observed in HMBC were effectively used to resolve any ambiguity in accurate assignments. **a** C5 was assigned 73.32 ppm as it showed a strong HMBC connectivity to **a** H1 (Fig. 2) and a weak cross peak to **a** H6 (not shown in Fig. 2). **d** H4 at 3.57 ppm similarly gave a connectivity to resonance at 73.40 ppm, establishing it to be **d** C3. Also, the **d** H3/**d** C2 and **d** H3/**d** C4 correlations observed in HMBC (Fig. 2), further support **d** H3 assignment. **a** H6 was similarly found to overlap with **b** H2; as a result ^{13}C resonance assignments for **a** C6 and **b** C2 could not be obtained directly from the single bond correlation spectrum. However, a resonance at 60.89 ppm was assigned **a** C6 as it showed a weak HMBC coupling to **a** H4 (not shown in Fig. 2). Assignment of **b** C2 at 68.21 ppm was facilitated by two HMBC connectivities observed for **b** C2 with both **b** H3 (3.88 ppm) and **b** H4 at 4.21 ppm. Also, **a** H6 was found to show weak connectivities (not shown in Fig. 2) to both **a** C5 and **a** C4 (Table 2), while **b** H2 at 3.79 ppm was coupled to **b** C3 at 80.24 ppm (Fig. 2), eliminating any ambiguity in assigning **a** H6 and **b** H2.

Amide Resonance Assignment: While these data locate the positions and assignments of all the carbon-bound protons, assignment of the 1H resonances of the amides was necessary to ascertain the location of the amino acid in the structure. To this end, spectra were recorded in H_2O with water suppression where three amide proton signals were observed. Two were assigned to the

amides of the two acetamido sugars **a** and **d** by coupling correlation to the respective H2 signals (3.62 ppm and 3.67 ppm) in water suppressed DQF-COSY spectra (not shown). The third at 7.78 ppm was assigned to serine because it was coupled to its α -proton (discussed below). Results of water suppressed HOHAHA with two different spin lock mixing times are listed in Table 2, showing connectivities from labile protons. When a short mixing time (20 ms) is used, the amide resonance at 7.78 ppm, **d** H_N, shows strong correlations to **d** H2 and **d** H3, and weak correlations to **d** H4 and **d** H1. It has been observed that the amide resonance gives strong NOE to its methyl protons across the carbonyl functionality in an N-acetyl moiety [26]. Water suppressed NOESY (not shown) with a mixing time of 200 ms shows an intense cross peak between **d** H_N and a methyl resonance at 2.02 ppm, clearly establishing the respective assignments of the amide proton and the methyl protons for the N-acetyl group of residue **d**. HMQC directly gives the ¹³C chemical shift (23.48 ppm) for this methyl resonance. Also, this same methyl proton resonance shows a strong correlation to carbonyl carbon resonance at 174.80 ppm in SELHMBC and in HMBC (Fig. 2). This confirms **d** to be β -GlcNAc. Similar observations show the N-acetylation of muramic acid and provide complete resonance assignments of its N-acetyl moiety.

Linkage Assignments: Because the ¹H and ¹³C resonances of all four residues have been completely assigned, HMBC (Fig. 2) was effectively used [27] for unambiguous assignment of inter-glycosidic linkages. Cross peaks were observed between all the anomeric protons and the linkage carbon atoms. In addition, HMBC cross peaks were observed between the anomeric carbon resonances of residues **a**, **c** and **d** and the proton of the aglycone linkage. Thus residues **b**, **c** and **d** form the backbone of the repeating sub-unit while residue **a** forms a side chain with **b** as indicated in the structural

formula of Scheme 1. The inter-residue NOESY cross peaks across each of these glycosidic linkages (Fig. 3) further support the proposed sequence [28].

Non Carbohydrate Moiety: The four sugars of the repeating subunit account for most of the signal intensity from carbon-bound protons in the HMQC spectrum of Fig. 1. But three distinct peaks remain, two of which are methylene signals both coupled to a methine proton. All the ^1H and ^{13}C chemical shifts are consistent with a serine residue [29] which was also detected in the amino acid analysis. Signal integration of 1D- ^1H shows comparable intensity of the H_α resonance at 4.40 ppm with the resolved anomeric protons. H_α of serine (**s** H_α) shows vicinal coupling to the resonance of the amide proton at 7.87 ppm in water suppressed DQF-COSY. As indicated in Table 2, this same resonance shows connectivities to all resonances of the serine spin system in water suppressed HOHAHA, clearly indicating its assignment to the amide proton of serine (**s** H_N). The amide proton of serine in water suppressed NOESY (not shown) shows NOE correlation to **b** H5, consistent with the amide linkage of serine to GalA (residue **b**) [30]. Furthermore, substitution of C6 of GalA was evident from the negative α -effect on the carbonyl ^{13}C chemical shift of C6 [31-32] as compared to unsubstituted GalA [33].

Absolute Configuration: Comparison of GLC retention times of the trimethylsilyl derivatives of the 2-butyl glycosides of GlcNAc and rhamnose with that of authentic reference compounds [34-35] established their absolute configuration as **D** and **L** respectively. Analysis of the GLC data for GalA and MurNAc included glycosides with both resolved isomers of 2-butanol as well as the racemic alcohol in order to be sure of the assignment of the absolute configuration of these sugars. Both the N-acetylated and de-N-acetylated forms of muramic acid were used as standards to identify both forms of the

sugar resulting from acidic solvolysis. All these GC data supported assignment of the D absolute configuration to both residues in spite of the NOE data reported in Fig. 3 which show that the NOE intensity from **a** H1 to **b** H3 is much more intense than the **a** H1/**b** H4 cross peak. Such a pattern of NOE has been widely used to infer that sugars with the α -linkage to the 3-position of a Gal residue must have *opposite* absolute configurations [36-37]. We conclude that there must be some unusual feature of the 3-dimensional conformation of this polysaccharide which leads to departures from this well established rule.

Smith Degradation: The structure of the repeating subunit of the CPS (Scheme 1) indicates that only one sugar in the repeating oligosaccharide should be susceptible to cleavage by Smith Degradation, namely, the 4-linked rhamnosyl residue (**c**). Hence, the CPS was subjected to Smith degradation [38-39] and the resulting Smith oligosaccharide (SMOS) was purified and isolated by gel-filtration chromatography using Bio-Gel P-2.

Carbohydrate analysis using acid hydrolysis followed by anion exchange chromatography of SMOS showed the presence of only glucosamine, muramic acid and galacturonic acid, clearly showing the absence of rhamnose in the SMOS. Also, the HMQC spectrum (not shown) shows that SMOS has only three rather than four anomeric resonances, though it does have all three amide resonances (data not shown) and four methyl proton resonances as in the CPS, indicating the cleavage of only rhamnose and giving rise to 4-deoxytetritol moiety (**t**).

All proton assignments (Table 5) for SMOS were obtained from a series of HOHAHA experiments carried out with incremental spin lock mixing times. Appearance of sequential connectivities from a well resolved resonance such as the anomeric or methyl resonance was used for assigning the rest of the

resonances in a given spin system. ^{13}C resonance assignments were obtained from HMQC spectra and ambiguities in assignments were resolved with the aid of HMBC data (Table 4).

As in the case of the CPS, long range HMBC cross peaks were observed between all anomeric protons and linkage carbon resonances including the linkage to the deoxytetritol moiety (**t**) (Table 4). Also, the anomeric carbon resonances of residues **a** and **d** show correlations to the respective proton at the aglycone linkage confirming all the linkage assignments.

Mass spectra of SMOS confirmed the attachment of serine to the GalA residue. The matrix assisted laser desorption (MALDI) spectrum of the Smith oligosaccharide gives primarily the $(M + Na)^+$ and $(M + 2Na - H)^+$ ions at m/z values of 870.5 and 892.6 (data not shown). The $(M + Na)^+$ ion was chosen to probe the structure of this molecule by high energy collision-induced dissociation (CID) in the first field free region of a double focusing mass spectrometer, and the CID spectrum of that is shown in Fig. 4. The ions at m/z 666 and 594 are formed by the losses of 204 and 276 from the precursor ion which can be rationalized to the presence of an N-acetyl hexosamine (HexNAc) and a muramic acid (MurNAc) residue in the molecule. The ion at m/z 392 can be explained by loss of 276 from the ion at m/z 666 and/or loss of 204 from the ion at m/z 594. Consequently, the ions at m/z 666, 594 and 392 reveal that the HexNAc and MurNAc moieties are linked independently to the molecule and these are at the termini of the molecule. Similarly, the presence of terminal serine and tetritol groups is shown by the fragment ions at m/z 782 and 766, as these ions are formed by loss of 88 (serine) and 104 (tetritol) from the precursor ion. Based on the knowledge of ions formed and the neutral species lost in the CID spectrum of $(M + Na)^+$ ion, the remaining part of the molecule was predicted to be a hexuronic acid

moiety to which all the above groups are linked. The mass spectral fragmentation (Fig. 4) shows unambiguously that these four residues are attached to galacturonic acid.

V. Discussion

While the chemical structures of the repeating subunits of the capsular polysaccharides of *V. vulnificus* strains MO6-24 and BO62316 are somewhat similar, the structure which we propose for the capsular polysaccharide of *V. vulnificus* ATCC 27562 differs in a more fundamental way from that of the other two strains. All three structures feature a uronic acid with the D-*galacto* configuration as the branch point of the tetrasaccharide repeating subunit. But the latter two structures have D-GalNAcA while the present one has D-GalA with the serine amide substitution. Residues of L-QuiNAc (N-acetyl quinovosamine) in the main backbone of the MO6-24 structure are replaced by L-Rha and by D-GalNAc in the present structure and the linkages are α -(1 \rightarrow 4)-rather than α -(1 \rightarrow 3)-. The side chain L-QuiNAc of MO6-24 is replaced by the residue of muramic acid in the ATCC 27562 structure. All three strains are pathogenic, having been isolated from sera of infected patients from California, Maryland and Florida respectively. Examination of the chemical structure does not reveal any common feature which may be correlated with pathogenicity [10]. Our survey of the capsular polysaccharides of a number of clinical and environmental strains by HPAEC analysis of carbohydrate composition indicates that there are likely to be a wide variety of different structures which are associated with pathogenic strains. Simple carbohydrate analysis does not reveal any obvious trends which can be used to distinguish clinical from environmental strains. Detailed structures of most of these capsular polysaccharides are not known and no attempts at detailed molecular modeling of these structures have been reported. Such

efforts would apparently be required to discover whether there is some underlying common three-dimensional feature which can be correlated with biological activity.

While muramic acid is commonly found in the peptidoglycan of bacterial cell walls, it has not been widely found in other bacterial polysaccharides such as LPS or CPS. [40]. The report of muramic acid in the LPS O-chain of *Yersinia ruckerii* is the only one known to us [41]. 3-O-(S)-1-carboxyethyl-D-GlcNAc (isomuramic acid) has been reported in LPS of *Proteus penneri* strains 19, 35 and 62 [11,24]. Related derivatives, such as 4-O-1-carboxyethyl derivatives of glucose or glucosamine with both the R and S configuration have been identified in the O-antigenic components of many gram negative types. Knirel and co-workers used cation exchange chromatography to identify isomuramic acid [11]. We show here that anion exchange chromatography using PAD can be used to distinguish muramic from isomuramic acid with differences in retention time sufficiently large that a standard isomuramic acid is unnecessary.

Uronic acid amides of of serine, threonine, lysine, glutamate and alanine have been reported in some capsular polysaccharides of *H. influenza*, [42] *Klebsiella*, [43] and *E. coli* [44-45] as well as in LPS O-chains of *P. mirabilis* [31,46]. Also primary amides have been reported in several capsular polysaccharide structures [30] and we have found a uronic acid primary amide in the capsule of *V. vulnificus* strain 6353 (Reddy et al, unpublished results). The modification of the uronic acid by serine was suggested by our analysis of the NMR data in which all the signals of the CH pairs in HMQC spectrum (Fig. 1) were assigned to parts of the structure. The mass spectral data on the trisaccharide alditol product of Smith degradation provided further support for the proposal of the serine amide and the amide proton NMR spectra

provided more detailed information. In specific, the NOESY spectrum of the amide resonances supported linkage to uronate by observation of a cross peak between amide proton assigned to the serine amide and H5 of GalA.

Amide proton NMR spectra, which are crucial to modern applications in protein NMR spectroscopy, are especially useful for polysaccharides from marine bacteria which are rich in nitrogen and contain many amino sugars acylated in various ways. All amino sugars were shown to be N-acetylated in this structure by the amide proton spectra. Most common amide proton resonances, such as those of GlcNAc, GalNAc etc. appear near 7.8 to 8.5 ppm but the chemical shift of the amide in MurNAc is far downfield at 10.8 which is unusual for acetamido sugars.

Acknowledgment

We thank Dr. Yuriy Knirel for generously providing a sample of the *P. penneri* strain 19 O-chain as a source of isomuramic acid.

References:

1. A.C. Wright, R.T. Hill, J.A. Johnson, M.C. Roghman, R.R. Colwell and J.G. Morris *Appl. Environ. Microbiol.* 62 (1996) 717-724.
2. A.C. Wright, L.M. Simpson, J.D. Oliver, and J.G. Morris, *Infect. Immun.* 58 (1990)1769-1773.
3. J.L. Powell, A.C. Wright, S.S. Wasserman, D.M. Hone, and J.G. Morris, *Infec. Immun.* 65, (1997) 3713-3718.
4. S.J.N. Devi, U. Hayat, C.E. Frasch, A.S. Kreger, and J.G. Morris, *Infect. and Immun.* 63 (1995) 2906-2911.
5. S.J.N. Devi, U. Hayat, J. L. Powell, and J.G. Morris, *Infect. Immun.* 64 (1996) 2220-2224.
6. G.P. Reddy, U. Hayat, C. Abeygunawardena, C. Fox, A.C. Wright D.R. Maneval, C.A. Bush, and J.G. Morris, *J. Bacteriol.* 174 (1992) 2620-2630.
7. U. Hayat, G.P. Reddy, C.A. Bush, J.A. Johnson, A.C. Wright, and J.G. Morris, *J. Infect. Dis.* 168 (1993) 758-762.
8. J.G. Simonson, and R.J. Siebeling, *Infect. and Immun.* 61 (1993) 2053-2058.
9. G.P. Reddy, U. Hayat, C.A. Bush and J.G. Morris *Anal. Biochem.* 214 (1993) 106-115.
10. C. A. Bush, P. Patel, S. Gunawardena, J.L. Powell, A. Joseph, J.A. Johnson and J. G. Morris *Anal. Biochem.* 250 (1997) 186-195

11. S.N. Senchenkova, A.S. Shashkov, Y.A. Knirel, N.K. Kochetkov, K. Zych and Z. Sidorczyk *Carbohydr. Res.* 293 (1996) 71-78.
12. M.R. Hardy and R.R. Townsend *Meth. Enzymol.* 230 (1994) 208-225.
13. A. Bax, and D.G. Davis, *J. Magn. Reson.* 65 (1985) 355-360.
14. D.G. Davis and A. Bax *J. Am. Chem. Soc.* 107 (1985) 2820-2821.
15. A. Bax, R.H. Griffey, and B.L. Hawkins, *J. Magn. Reson.* 55 (1983) 301-315.
16. A. Bax, and M.F. Summers, *J. Am. Chem. Soc.* 108 (1986) 2093-2094.
17. P.J. Hore, *J. Magn. Reson.* 55 (1983) 283-300.
18. S.C. Brown, P.L. Weber, and L. Mueller, *J. Magn. Reson.* 77 (1988) 166-169.
19. K.S. Sato, T. Asada, M. Ishihara, F. Kunihiro, Y. Kammei, E. Kubota, C.E. Costello, S.A. Martin, H.A. Scoble, and K. Biemann *Anal. Chem.* 59 (1987) 1652-1659.
20. V.S. Kumar Kolli, and R. Orlando, *Rapid Commun. Mass Spectrom.* 10 (1996) 923-926.
21. V.S. Kumar Kolli, and R. Orlando, *Anal. Chem.* 69 (1997) 327-332.
22. C. Abeygunawardena, and C.A. Bush, *Advan. Biophys. Chem.* 3 (1993) 199-249.
23. D. Uhrin, J.R. Brisson, L.L. Maclean, J.C. Richards and M.B. Perry, *J. Biomol. NMR* 4 (1994) 615-630.

24. Y.A. Knirel, N.A. Paramonov, E.V. Vinogradov, A.S. Shashkov, N.K. Kochetkov, Z. Sidorczyk, and A. Swierzko, *Carbohydr. Res.* 235 (1992) C19-C23.
25. K. Bock, I. Lundt, and C. Pedersen, *Tetrahedron Lett.* 13 (1973) 1037-1040.
26. P. Cagas, K. Kaluarachchi, and C.A. Bush, *J. Am. Chem. Soc.* 113 (1991) 6815-6822.
27. L. Lerner and A. Bax, *Carbohydr. Res.* 166 (1987) 35-46.
28. J.H. Prestegard, T.A.W. Koerner, P.C. Demou, and R.K. Yu *J. Am. Chem. Soc.* 104 (1982) 4993-4995.
29. A.D. Kline and K. Wuthrich *J.Mol. Biol.* 192 (1986) 869-890.
30. I. Sadvskaya, J.R. Brisson, E. Altman, and L. M. Mutharia, *Carbohydr. Res.* 283 (1996) 111-127.
31. J. Radziejewskalebrecht, A.S. Shashkov, E.V. Vinogradov, H. Grosskurth, B. Bartodziejska, A. Rozalski, W. Kaca, L.O. Kononov, A.Y. Chernyak, H. Mayer, Y.A. Knirel, and N.K. Kochetkov, *Eur. J. Biochem.* 230 (1995) 705-712.
32. Z. Sidorczyk, A. Swierzko, Y.A. Knirel, E.V. Vinogradov, A.Y. Chernyak, L.O. Kononov, M. Cedzynski, A. Rozalski, W. Kaca, A.S. Shashkov, and N.K. Kochetkov, *Eur. J. Biochem.* 230 (1995) 713-721.
33. K. Bock, and C. Pedersen, *Advan. Carbohydr. Chem. Biochem.* 41 (1983) 27-66.

34. G.J. Gerwig, J.P. Kamerling, and J.F.G. Vliegthart, *Carbohydr. Res.* 62 (1978) 349-357.
35. G.J. Gerwig, J.P. Kamerling, and J.F.G. Vliegthart, *Carbohydr. Res.* 77 (1979) 1-7.
36. G.M. Lipkind, A.S. Shashkov, S.S. Mamyán, and N.K. Kochetkov, *Carbohydr. Res.* 181 (1988) 1-12.
37. H. Baumann, P.E. Jansson, and L. Kenne *J. Chem. Soc. Perkin Trans.* 1 (1988) 209-217.
38. I.J. Goldstein, G.W. Hay, B.A. Lewis, and F. Smith *Meth. Carbohydr. Chem.* 5 (1965) 361.
39. A.M. Wu, E.A. Kabat, M.E.A. Pereira, F.G. Gruezo, and J. Liao, *Arch. Biochem. Biophys.* 215 (1982) 390-404.
40. L. Kenne, and B. Lindberg, "Bacterial polysaccharides." in *The Polysaccharides* vol. 2, pp. 287-363, G.O. Aspinall, ed. Academic Press, N.Y. (1983) 287-363.
41. J.H. Banoub, D.H. Shaw, H. Pang, J.J. Krepinisky, N.A. Nakhla, and T. Patel, *Biomed. Environ. Mass Spec.* 19 (1990) 787-790.
42. P. Branefors-Helander, L. Kenne, B. Lindberg, K. Petersson, and P. Unger *Carbohydr. Res.* 97 (1981) 285-291.
43. P.E. Jansson, B. Lindberg, G. Widmalm, G.G Dutton, A.V. Lim, and I.W. Sutherland, *Carbohydr. Res.* 175 (1988) 103-109.
44. T.Dengler, B. Jann, and K. Jann, *Carbohydr. Res.* 150 (1986) 233-240.

45. P.Hofmann, B. Jann, and K. Jann, *Carbohydr. Res.* 139 (1985) 261-271.
46. W. Gromska, and H. Mayer, *Eur. J. Biochem.* 62 (1976) 391-399.

VII. Legends for Figures and Scheme

- Figure 1. ^{13}C -decoupled, ^1H detected multiple quantum correlation ($^1\text{H}[^{13}\text{C}]\text{HMQC}$) spectrum from the capsular polysaccharide of *V. vulnificus* ATCC 27562. The inset shows the cross-peaks in the upfield methyl region.
- Figure 2. ^1H - ^{13}C multiple-bond correlation ($^1\text{H}[^{13}\text{C}]\text{HMBC}$) spectrum of the capsular polysaccharide. The two delays were $\Delta_1 = 3.3$ ms and $\Delta_2 = 45.0$ ms. For simplicity we have avoided using lower case bold-face letter notation twice to indicate residues in a given cross peak as used in the text, except for inter-residue correlation peaks. Thus, H1/**a**5 indicates **a** H1/**a** C5 and **a**H1/**b**3 indicates **a** H1/**b** C3, etc. Weak cross peaks (**a** H4/**a** C6, **a** H6/**a** C4, **a** H6/**a** C5, **d** H4/**d** C3 and **d** H4/**d** C5) are not observable at this contour level. The inset shows the long range connectivities to the upfield methyl proton resonances. Peaks marked with an asterisk are folded in the ^{13}C dimension.
- Figure 3. Partial NOESY spectrum of the capsular polysaccharide with a 60 ms mixing time. Only the NOE cross peaks from the anomeric and **s**- α resonances are labeled. For simplicity **a** H1 is labeled **a**1, etc.
- Figure 4. MALDI-MS/MS CID spectrum of $(\text{M}+\text{Na})^+$ ion of Smith oligosaccharide; inset shows the fragmentation pattern of $(\text{M}+\text{Na})^+$ ion.
- **Scheme 1.** Structure of CPS of *V. vulnificus* ATCC 27562.